TISSUE ENGINEERING: Part A
Volume 20, Numbers 3 and 4, 2014

DOI: 10.1089/ten.tea.2013.0108

New Bio-Ceramization Processes Applied to Vegetable Hierarchical Structures for Bone Regeneration: An Experimental Model in Sheep

Giuseppe Filardo, MD,[1] Elizaveta Kon, MD,[1] Anna Tampieri, PhD,[2] Rafael Cabezas-Rodríguez, MSc,[3] Alessandro Di Martino, MD,[1] Milena Fini, MD,[4,5] Gianluca Giavaresi, MD,[4,5] Marco Lelli, MSc,[6] Julian Martínez-Fernández, PhD,[3] Lucia Martini, DVM,[4,5] Joaquin Ramírez-Rico, PhD,[3] Francesca Salamanna, PhD,[4] Monica Sandri, PhD,[2] Simone Sprio, PhD,[2] and Maurilio Marcacci, MD[1]

Bone loss is still a major problem in orthopedics. The purpose of this experimental study is to evaluate the safety and regenerative potential of a new scaffold based on a bio-ceramization process for bone regeneration in long diaphyseal defects in a sheep model. The scaffold was obtained by transformation of wood pieces into porous biomorphic silicon carbide (BioSiC®). The process enabled the maintenance of the original wood microstructure, thus exhibiting hierarchically organized porosity and high mechanical strength. To improve cell adhesion and osseointegration, the external surface of the hollow cylinder was made more bioactive by electrodeposition of a uniform layer of collagen fibers that were mineralized with biomimetic hydroxyapatite, whereas the internal part was filled with a bio-hybrid HA/collagen composite. The final scaffold was then implanted in the metatarsus of 15 crossbred (Merinos-Sarda) adult sheep, divided into 3 groups: scaffold alone, scaffold with platelet-rich plasma (PRP) augmentation, and scaffold with bone marrow stromal cells (BMSCs) added during implantation. Radiological analysis was performed at 4, 8, 12 weeks, and 4 months, when animals were sacrificed for the final radiological, histological, and histomorphometric evaluation. In all tested treatments, these analyses highlighted the presence of newly formed bone at the bone scaffolds' interface. Although a lack of substantial effect of PRP was demonstrated, the scaffold + BMSC augmentation showed the highest value of bone-to-implant contact and new bone growth inside the scaffold. The findings of this study suggest the potential of bio-ceramization processes applied to vegetable hierarchical structures for the production of wood-derived bone scaffolds, and document a suitable augmentation procedure in enhancing bone regeneration, particularly when combined with BMSCs.

Introduction

A bone defect can be caused by several pathological conditions (bone tumors, infections, major trauma with bone loss…) or by surgical procedures,[1] and the associated loss of function considerably impairs the quality of life of the affected patients.[2] Unfortunately, extensive bone loss or destruction is still a major problem in orthopedics, due, in large part, to the lack of predictability in obtaining functional bone reconstruction.[1,3–9]

Bone tissue engineering offers a promising strategy for healing severe bone injuries by utilizing the body's natural biological response to tissue damage in conjunction with engineering principles.[10] The limiting factor is represented by the insufficient strength of currently available scaffolds, although so far a good compromise in terms of mimicking the micro- and macro-porosity of natural bone was reached.[11–13] Indeed, the remarkable biomechanical properties of bone depend on its hierarchically organized structure, from the molecular to nano-, micro-, and macro-scales, which make it able to constantly adapt to ever-changing mechanical needs.[14,15] In this regard, only scaffolds endowed with a hierarchically organized structure can exhibit complex biomechanical performances that are able to activate mechanotransduction processes, yielding regeneration of well-organized bone.

[1]Laboratory of Biomechanics, Rizzoli Orthopaedic Institute, Bologna, Italy.
[2]Institute of Science and Technology for Ceramics, National Research Council, Faenza, Italy.
[3]Departamento Física de la Materia Condensada—ICMS, Universidad de Sevilla, CSIC, Seville, Spain.
[4]Laboratory of Biocompatibility, Technological Innovations and Advanced Therapies, Department Rizzoli RIT, Rizzoli Orthopedic Institute, Bologna, Italy.
[5]Laboratory of Preclinical and Surgical Studies–Rizzoli Orthopedic Institute, Bologna, Italy.
[6]Department of Chemistry G. Ciamician, University of Bologna, Bologna, Italy.

Natural woods manifest behavior similar to bones in terms of elasticity, lightness, and strength. In this regard, some woods can be transformed into porous devices acting as scaffolds and exhibiting pore size and organization that are suitable to mimic the biomechanical characteristics of human bone.[16–18]

The purpose of this experimental study is to evaluate the safety and regenerative potential of a new scaffold based on a bio-ceramization process[16,17,19] for bone regeneration in long diaphyseal defects in a sheep model. The scaffold was obtained by the transformation of wood pieces into porous biomorphic silicon carbide (BioSiC®). The process enabled the maintenance of the original wood microstructure, thus exhibiting hierarchically organized porosity and high mechanical strength. Natural woods manifest behavior similar to bones in terms of elasticity, lightness, and strength; therefore, by translating its structure into bioactive, highly porous scaffolds, a bone substitute prototype exhibiting both the biochemical and biomechanical characteristics of human bone has been developed. Its microstructure can mimic the cortical part of bone; in this regard, to provide increased biomimesis with bone and improved osteoconductivity, the scaffold was conceived and designed as a bi-layer device. It was made of an external, cortical-like, shell represented by BioSiC, and a spongy-like core, made of a highly bioactive hybrid composite obtained by a biologically inspired process of self-assembling and mineralization of a collagen matrix with nano-nuclei of Mg- and CO_3- co-substituted hydroxyapatite.[20–24] In addition, since no single approach can successfully meet all the demands of bone regeneration alone and the concept of providing a combination of the key elements for tissue healing (an osteoconductive matrix, osteogenic cells, and growth factors) is commonly proposed in the scientific community, it was also tested whether loading autologous cells (bone marrow stromal cells [BMSCs]) or growth factors (derived from platelet rich plasma [PRP]) on the scaffold might enhance the repair process. An emerging option to provide viable osteogenic cells directly in the open theatre, with no need of cell expansion, and therefore lower costs and regulatory limitations, is the use of autologous bone marrow concentrate.[25] This overcomes long-lasting and expensive *in vitro* culture expansion, avoiding the possibility of transformation of the cell phenotype and overcoming the strict rules on cell manipulation that, requiring a Good Manufacturing Practice facility in processing and isolating MSCs for clinical applications, greatly limit their use. Despite the fact that quality parameters cannot be reliably predicted, some publications indicate that, compared with the transplantation of a defined type of cell, applying mixed populations of mesenchymal and hematopoietic progenitor cells at different stages of differentiation is more effective for osteogenic regeneration.[26,27] Thus, we applied this cell population to the scaffold to increase the regeneration process. Another possibility for favoring bone regeneration is the application of growth factors, which are expressed during different phases of tissue healing and are, therefore, a key element to promote tissue regeneration.[28] In fact, growth factors carried out on orthopedic devices have been reported to enhance osteoblastic activity and thus bone regeneration.[29,30] Platelets participate predominantly in the early regeneration phases and, by degranulating, they produce a great number of growth factors that initiate and maintain the healing process.[31,32] PRP is an inexpensive way to obtain many platelets and therefore many growth factors, and it has already been largely applied as a carrier of growth factors in different fields of medicine.[33–35] Nevertheless, the existing data in preclinical and clinical studies are controversial; results can be seen only at certain concentrations and even detrimental effects have been reported.[36–42] Therefore, we decided to test the potential of this biological strategy for tissue-healing enhancement on this new scaffold in the big animal model, in order to have clear indications on the most suitable augmentation approach for a future clinical application.

Materials and Methods

Scaffold development

Cortical-like part. The cortical-like part of the scaffold was manufactured as a hollow cylinder (external diameter: 15 mm; internal diameter: 9 mm; height: 20 mm) made of porous silicon carbide (BioSiC). The scaffold was obtained by biomorphic transformation of Sipo wood (*Entandophragma utile*), following a procedure reported elsewhere.[43] In brief, blocks of Sipo wood were pyrolized by heating at 800°C under a flowing argon atmosphere (0.5°C/min heating rate) to obtain a wood-derived carbon template (Fig. 1b) that was subsequently machined to a hollow cylinder using a lathe. The morphology of Sipo wood is characterized by oriented porosity; hence, in order to improve the cell conduction within the scaffold thus favoring osteointegration and physical stabilization of the bone-implant interface, the scaffold was developed by cutting wood sources so as to keep pores exposed toward the bone (Fig. 1a–e). Then, the pyrolyzed wood was melt-infiltrated with silicon (Silgrainc HQ −99.7% purity) by heating for more than 1450°C in a vacuum furnace. An Si/C weight ratio of 3.2 was used to ensure a complete conversion of C to SiC. The obtained material consisted of a porous ceramic SiC scaffold mimicking the original wood structure, with residual Si filling some of the pores (Fig. 1c). Residual Si was removed by wet chemical etching using an HF/HNO_3 mixture at a molar ratio of 1.66 in water under stirring, to obtain a hollow, porous SiC cylinder with elongated porosity (Fig. 1d).

The resulting bioSiC scaffolds had an average apparent density of $(1.77 \pm 0.08)\ g \cdot cm^{-3}$, with a porosity estimated as 45% volume by geometrical arguments. An image analysis of transverse sections showed a bimodal pore distribution of approximately 40% large diameter pores ($150 \pm 20\ \mu m$) and 60% small diameter pores ($7 \pm 3\ \mu m$). Figure 2 describes the mechanical strength of the porous Sipo-derived scaffold versus porosity, as well as a morphological comparison between the starting wood and the final SiC scaffold.

To improve cell adhesion and osseointegration, the external surface of the hollow cylinder was made more bioactive by electrodeposition of a uniform layer of collagen fibers that were mineralized with biomimetic hydroxyapatite.[44] The electrodeposition process was carried out in a two-electrode cell, where a work electrode (cathode) was constituted by the BioSiC shell and the counter-electrode (anode) was constituted by a platinum filament. The electrodes were immersed into a cell containing a mixture of aqueous solutions and a collagen suspension, prepared as follows. Solution A: dissolution of $Ca(NO_3)_2$ in distilled water for an approximate concentration of Ca^{2+} of 42 mM. Solution B: dissolution of $NH_4H_2PO_4$ in distilled water for an approximate concentration of PO_4^{3-} of 25 mM. The suspension of Type I collagen was prepared starting by Achille's tendon of

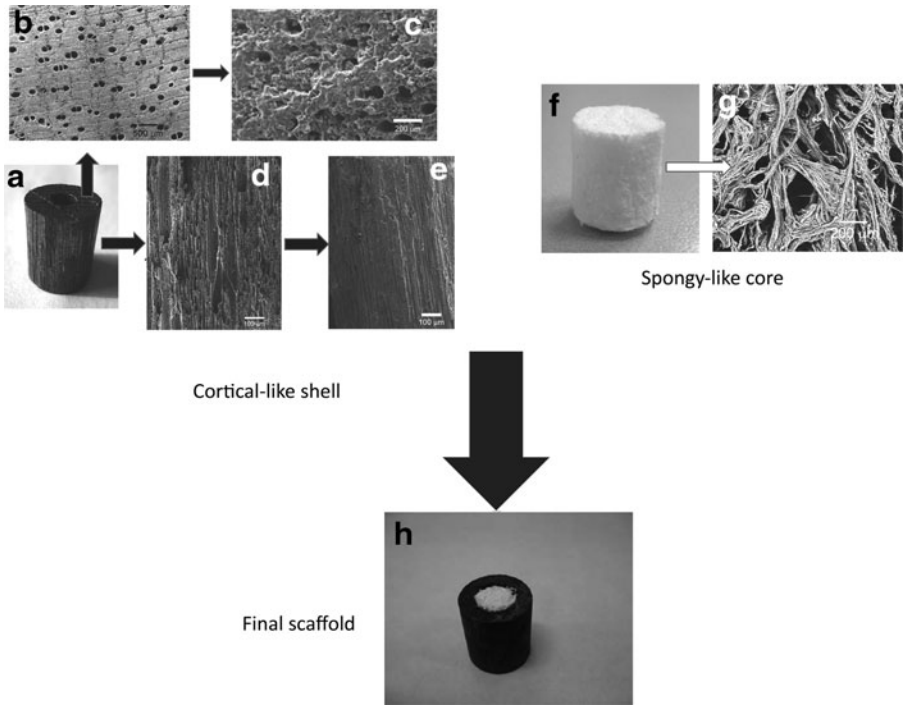

FIG. 1. BioSiC(HaCol) scaffold design. **(a–e)** Puts in evidence the complex microstructure of the external shell made of Sipo-derived SiC, particularly evidencing the oriented porosity **(b, d)**, and the alteration of the surface due to the coating **(c, e)**. **(f, g)** Highlights the structure of the spongy part of the scaffold. **(h)** Shows the final assembled scaffold: The load-bearing part is represented by the external shell, whereas the internal part is intended to promote osteoconductivity and bone regeneration due to the high biomimesis with bone (see Sprio *et al.*[21]).

horses following a proprietary method by Opocrin S.p.A.,[20] which enables to obtain a purified and telopeptide-free product in the form of a 1% (w/v) suspension.

The electro-deposition was carried out at 25°C with an applied constant galvanostatic current of 34 mA. The process allowed the fibration of collagen fibers and mineralization with nanonuclei of hydroxyapatite, during electrodeposition, with the formation of a uniform layer of mineralized collagen on the BioSiC scaffold; the layer thickness was related to the deposition time; in this regard, the deposition time was calibrated to achieve a coating of 50 μm in thickness.[44] After each deposition, the coated BioSiC was washed in distilled water and dried in air.

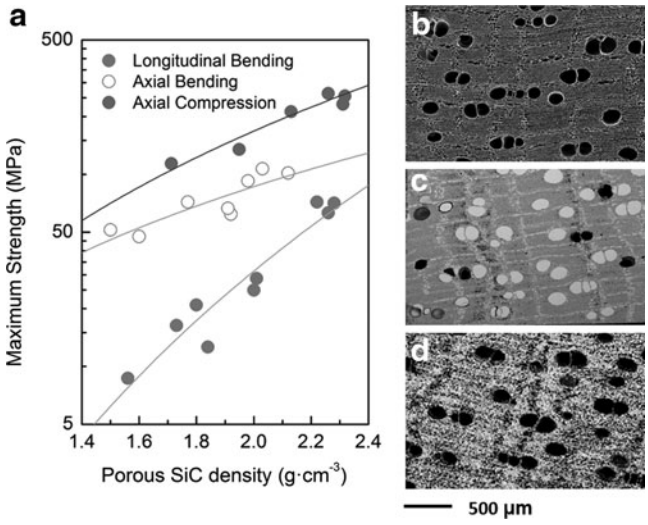

FIG. 2. **(a)** Mechanical strength of porous, Sipo-derived BioSiC in compression in the axial direction and in four-point bending in the axial and the transversal directions of the original wood pores. Compression data are from,[43] bending data are previously unpublished. **(b)** SEM micrograph of the carbon scaffold obtained from pyrolysis of Sipo Wood. **(c)** BioSiC/Si material obtained by infiltrating the previous scaffold with molten Si, and **(d)** BioSiC, a porous SiC ceramic mimicking the original wood precursor's microstructure.

Spongy-like part. Bio-hybrid HA/collagen composites were synthesized by neutralization of a suspension containing $Ca(OH)_2$ and $MgCl_2$ with acidic solution containing phosphoric acid and Type I collagen (OPOCRIN SpA). The variation of pH from 3.5 to 9–10 during the process enabled the assembling of collagen molecules into fibers, and simultaneous heterogeneous nucleation of biomimetic HA nanoparticles was achieved by pH variation, in the presence of Ca^{2+}, Mg^{2+}, CO_3^{2-}, and PO_4^{3-} ions.[20,21] The concentration of Ca^{2+} and PO_4^{3-} was adjusted to achieve the heterogeneous nucleation of the mineral phase in amounts mimicking the bone tissue (i.e., 70 wt%). The concentration of Mg^{2+} and CO_3^{2-} was adjusted to achieve ion content (in the site of calcium and phosphate, respectively) in biological-like amounts. The obtained gel was subjected to freeze drying and cut in the desired shape and size.

Assembling of the two components. The hollow BioSiC cylinder was filled with the bio-hybrid composite (Fig. 1). The fair elasticity of the spongy-like hybrid composite enabled its insertion in the hollow cylinder by press-fit, thus obtaining a stable bi-layered scaffold. The final scaffold, hereinafter referred to as BioSiC(HaCol), was sterilized by γ-ray irradiation at 25 kGy (GammaRad Italia SpA, Bologna, Italy).

Preparation of PRP

PRP was prepared as follows according to the method described in 2004 by Weibrich *et al.*[37]: Before scaffold

implantation (within about 2 h), ~20 mL of peripheral venous blood was collected into siliconized tubes containing 3.8% sodium citrate at a blood/citrate ratio of 9/1. PRP was obtained by two sequential centrifugations: at 200 *g* for 5 min and at 1000 *g* for 15 min. The number of platelets (PLTs) was determined on whole blood and on PRP under a microscope with a hemocytometer chamber after 1/100 dilution with 1% ammonium oxalate. The % yield was calculated in the following way: number of PLTs in PRP/number of PLTs in the whole blood × 100. Platelet number (mean ± SD) on whole blood was $348 \pm 145 \times 10^3/mm^3$ (range $250–560 \times 10^3/mm^3$); on PRP, it was $2018 \pm 851 \times 10^3/mm^3$ (range: $1200–3040 \times 10^3/mm^3$), with a mean % yield of 582% ± 119% (range 462%–745%). After platelet counting, the PRP was resuspended in platelet-poor plasma, so as to obtain a platelet concentrate equal to 1×10^6/mL plasma. For platelet activation, a sterile 10% solution of $CaCl_2$ (Sigma-Aldrich S.r.l., Milan, Italy) in the proportion 50 μL/mL was added to the PRP immediately before use and 2 mL of PRP were soaked into the scaffold.

Preparation of BMSCs

Before scaffold implantation, a 16-gauge bone-marrow needle was inserted into the posterior iliac crest. A 10-mL syringe was attached to the needle and a total bone marrow volume of 6–7 mL was collected in sterile vials containing 0.5 mL of 1:1000 heparin to prevent clotting, and was immediately processed by isopyknic centrifugation to concentrate the relatively few stem cells, thus improving bone marrow osteogenic efficiency. Briefly, an equal volume of phosphate-buffered saline (PBS) was added to the bone marrow, the mixture was then layered over undiluted Ficoll Paque (Sigma-Aldrich S.r.l.), which had a density of 1.083 g/mL and was centrifuged for 20 min at 400 *g*. The band of light-density cells was separated, washed, counted ($4 \pm 2 \times 10^6$ cells/mL), and resuspended in 200 μL of PBS for immediate implant. The whole procedure was performed under sterile conditions.

Study design

All *in vivo* experiments were performed in accordance with the European and Italian Law on animal experimentation and the principles stated in the "NIH Guide for the Care and Use of Laboratory Animals." The research protocol on animals was approved by the ethics committee of the Rizzoli Orthopaedic Institute and then by the Italian Ministry of Health.

Fifteen crossbred (Merinos-Sarda) adult sheep, aged 3.0 ± 0.5 years, 65 ± 5 kg b.w. (Pancaldi Raffele, Budrio, Bologna, Italy), after a quarantine period, were submitted to surgery. General anesthesia was induced with 6 mg/kg i.v. sodium thiopentone (2.5% solution) (Thiopental Inresa, Freiburg, Germany) and maintained with 60%/40% O_2/air 7 L/min and 2% isoflurane (Aerrane, Baxter SpA, Roma). All surgeries were carried out in aseptic conditions.

Each animal was placed on its left side, and the right hindlimb was shaved and disinfected. A medial approach to the metatarsus shaft was performed directly above the bone, and the medial aspect of the metatarsus was exposed. A 3.5-mm broad titanium dynamic compression plate with eight holes was contoured to the shaft; a high-speed perforator was used to drill the holes. The plate was fixed to the bone using 3.5 mm screws and distributing three screw holes distally and three proximally to the planned defect. Tapping and screw insertion was done manually. Thereafter, the defect was marked on the bone ensuring a standardized 2 cm defect between the fourth and fifth screw hole. The screws and plate were removed. The defect was cut with an oscillating saw under constant irrigation and preservation of soft tissues using two retractors inserted on both sides of the defect. The 2-cm segment was carefully removed; once the implant was applied, the screws were placed again in the proper site and the soft tissues were closed.

The created gap was treated according to the following three groups: In group 1, the scaffold was implanted alone (five sheep); in group 2, the scaffold was implanted with PRP augmentation (five sheep); and in group 3, BMSCs were added during implantation (five sheep). Then, a full cast was put on the treated leg. The sole of the claws was closed for 8 weeks, then left open to ensure weight bearing on the fracture site, but to prevent torsional or shear forces through the immobilization of the metatarsus shaft through the cast. At 12 weeks after surgery, the sheep were then let out to graze. The cast was changed twice at 4 and 8 weeks or on need (Fig. 3).

Radiographs of the operated limb were taken postoperatively at 4, 8, and 12 weeks (under sedation with ketamine and xylazine as described earlier) by means of a portable X-ray machine (Nessey HF30-Raffaello-ACEM SpA, Bologna, Italy).

Four months after surgery, the animals were pharmacologically euthanized with the i.v. administration of 10 mL mbutamide, mebenzonium iodine, and tetracaine chloride (Tanax; Hoechst, Frankfurt am Main, Germany), under general anesthesia. For each animal, the right metatarsus was excised and stripped of soft tissue; the presence of haematomas, oedema, and inflammatory tissue reactions were macroscopically evaluated. Then, bone segments were antero-posterior and medio-lateral radiographed, fixed in 4% buffered paraformaldehyde for 48 h, and processed for histological and histomorphometric investigations.

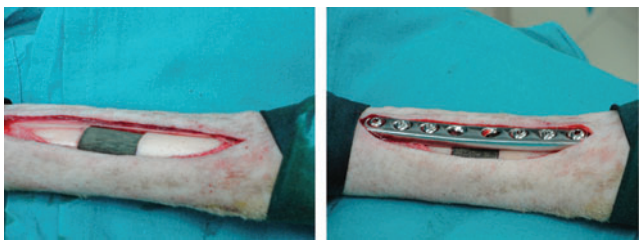

FIG. 3. Scaffold implantation procedure. Color images available online at www.liebertpub.com/tea

Radiological analysis

A score system was used to evaluate radiographs;[45] it ranges from 0 to 2 given for the proximal and distal osteotomy line in two different categories: osteotomy healing and periosteal callus presence. In the first category, 0 was assigned when there was discontinuity in the osteotomy line, 1 for continuity but the line was still visible, and 2 when the line was hardly recognizable. With regard to periosteal callus, 0 indicated no evidence of periosteal callus, 1 indicated

moderate presence, and 2 indicated marked/exuberant presence.

Histological and histomorphometric analyses

Undecalcified bone specimens were fixed in 4% paraformaldehyde, dehydrated in graded series alcohols, and embedded in poly-methyl methacrylate (Merck, Schuchardt, Hohenbrunn, Germany). Metatarsi were sectioned longitudinally and along a plane parallel to the long axis of the plate, respectively, using the same cutting-grinding system (EXAKT 400CS Micro Grinding System; EXAKT Apparatus GmbH, Norderstedt, Germany). Two sections for each sample were then automatically thinned to $80 \pm 10\,\mu m$ with a diamond grinding foil (ATM GmbH, Emil-Reinert-Str. 2, D-57636 Mammelzen), and subsequently polished (Struers Dap-7, Struers Tech, Denmark) to a thickness of $40 \pm 10\,\mu m$. Sections were stained with Toluidine Blue, Acid Fuchsin, Fast Green.

Bone histomorphometric measurements were performed semi-automatically inside and outside the scaffold in four equidistant regions of interest (2584×1936 pixels) (Fig. 4) by using an optic microscope (BX51; Olympus Optical Co., Europa GmbH, Germany) that was connected to an image analyzer system (Qwin; Leica Imaging Systems Ltd., Cambridge, United Kingdom) at $1.25\times$ magnification. To evaluate the scaffold osseointegration and healing bone process, the following static measurements were done:[46]

- Bone-to-implant contact (%): the amount of bone contact at the interface, defined as the percentage of implant perimeter showing a direct bone-to-implant contact without any intervening soft-tissue layers.
- New bone growth inside (%): the amount of new bone growth next to scaffold in an area located inside scaffold and expressed as a percentage.
- New bone growth outside (%): the amount of new bone growth next to scaffold in an area located outside scaffold and expressed as a percentage.

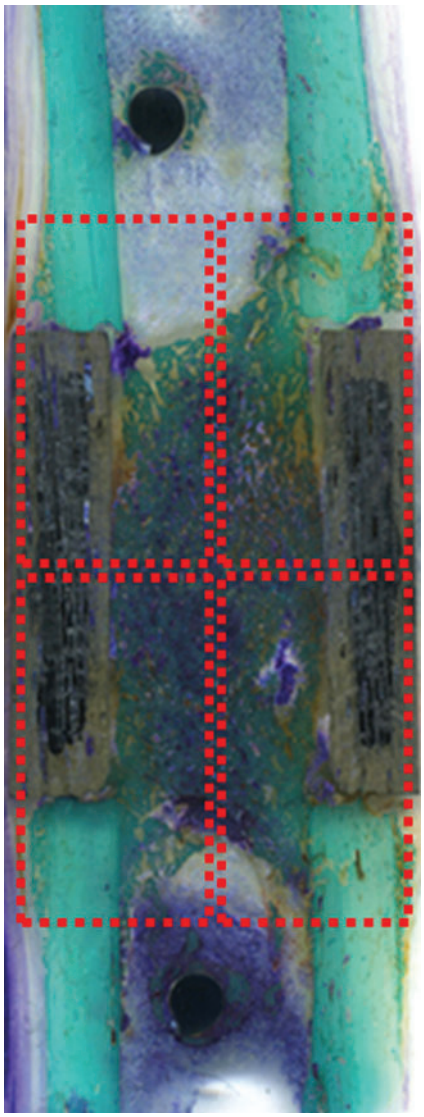

FIG. 4. Images of four equidistant region of interest (2584×1936 pixels—dashed rectangles) for the evaluation of histomorphometric measurements, performed inside and outside the scaffold: bone-to-implant contact (%), new bone growth inside (%), and new bone growth outside (%). Toluidine Blue, Acid Fuchsin, Fast Green staining. Scanner Epson 2480 Photo, Resolution 1200 dpi. Color images available online at www.liebertpub.com/tea

Statistical analysis

Statistical analysis was performed using the SPSS v.12.1 software (SPSS, Inc., Chicago, IL). Data are reported as mean ± SD at a significance level of $p < 0.05$. ANOVA followed by the Dunnett *t*-test was used to analyze data.

Results

Two sheep died postoperatively (one in BioSiC(HaCol) + PRP group and the other in BioSiC(HaCol) + BMSC group) for postoperative problems not related to implants. At euthanasia, macroscopic evaluation showed the implants to be in the proper position. There were no signs of inflammation or adverse tissue reaction in bone, peri-implant soft tissue, and/or integument associated with implants.

Radiological analysis

Osteotomy lines healed with time in BioSiC(HaCol) group, but were almost detectable at 16 weeks after surgery. The use of PRP or BMSCs did not further improve the osteotomy healing, where osteotomy lines were constantly and perfectly visible during time (Figs. 5 and 6a). The area of the periosteal callus increased over time in all groups (Figs. 5 and 6b). In the BioSiC(HaCol) group ($p < 0.005$), significant increases in the periosteal callus score were observed at 12 (2.0 ± 0.2) and 16 (2.0 ± 0.2) weeks after surgery in comparison with those at 4 (0.0) weeks. Apart from this, in the BioSiC(HaCol) + PRP and BioSiC(HaCol) + BMSC groups, significant increases in the periosteal callus score ($p < 0.005$ and $p < 0.05$, respectively) were observed at 12 [BioSiC(HaCol) + PRP: 1.5 ± 1.0; BioSiC(HaCol) + BMSC: 3.5 ± 0.5] and 16 [BioSiC(HaCol) + PRP: 2.5 ± 1.0; BioSiC(HaCol) + BMSC: 3.5 ± 0.5] weeks after surgery in comparison with those at 4 weeks [BioSiC(HaCol) + PRP: 0.0; BioSiC(HaCol) + BMSC: 1.0 ± 0.4]. Significantly higher values in periosteal callus score were found in BioSiC(HaCol) + BMSC group in comparison to BioSiC(HaCol)

($p < 0.05$) at 4 [BioSiC(HaCol) + BMSC: 1.0 ± 0.4; BioSiC(HaCol): 0.0] and 8 [BioSiC(HaCol) + BMSC: 2.8 ± 0.8; BioSiC(HaCol): 0.8 ± 0.4] weeks from surgery.

Histological and histomorphometric analyses

Histological evaluation showed neither inflammatory processes nor fibrous encapsulation at the bone-scaffold interface for all treatments.

Group 1: BioSiC(HaCol). BioSiC(HaCol) scaffolds presented dense and irregular connective tissue at the edges of the device characterized by a number of collagen fibers that clump together in bundles, sometimes accompanied by networks of elastic tissue. Newly formed bone tissue was present within the scaffold with an hourglass shape. The new bone was comparatively mature containing many bone lacunae. However, several areas of low bone-to-implant contact were observed on BioSiC(HaCol) surfaces (Fig. 7a).

Group 2: BioSiC(HaCol) + PRP. BioSiC(HaCol) scaffolds + PRP showed irregular dense connective tissue at the edge of the scaffold and between scaffold and cortical bone. The cortical areas in contact with the scaffold were spongy and eroded, with connective tissue interspersed with newly formed bone and small particles of the scaffold. The use of PRP improved the bone growth tissue inside the scaffold, and newly formed bone tissue was present within the scaffold. Nevertheless, areas of low bone-to-implant contact were also observed on BioSiC(HaCol) scaffolds + PRP surfaces (Fig. 7b).

Group 3: BioSiC(HaCol) + BMSCs. BioSiC(HaCol) scaffolds + BMSCs presented dense connective tissue at the edge of the scaffold, probably due to the persistence of bone callus, and newly formed bone tissue was present within the scaffold. Conversely to BioSiC(HaCol) and BioSiC(HaCol) + PRP (Fig. 7), BioSiC(HaCol) scaffolds + BMSCs exhibited a well-defined continuous layer of new bone. In addition, in comparison to BioSiC(HaCol) and BioSiC(HaCol) + PRP, bone osseointegration and remodeling processes were more evident with higher amounts of bone in contact with implants. In addition, the BioSiC(HaCol) scaffolds + BMSCs were partly covered with mineralized bone containing many bone lacunae and several osteoblasts (Fig. 7c).

Histomorphometric analyses provided a better comprehension of osseointegration and new bone formation processes (Table 1). In particular, Scheffé *post hoc* multiple comparison test highlighted differences in terms of bone-to-implant contact and new bone growth inside scaffold. Bone-

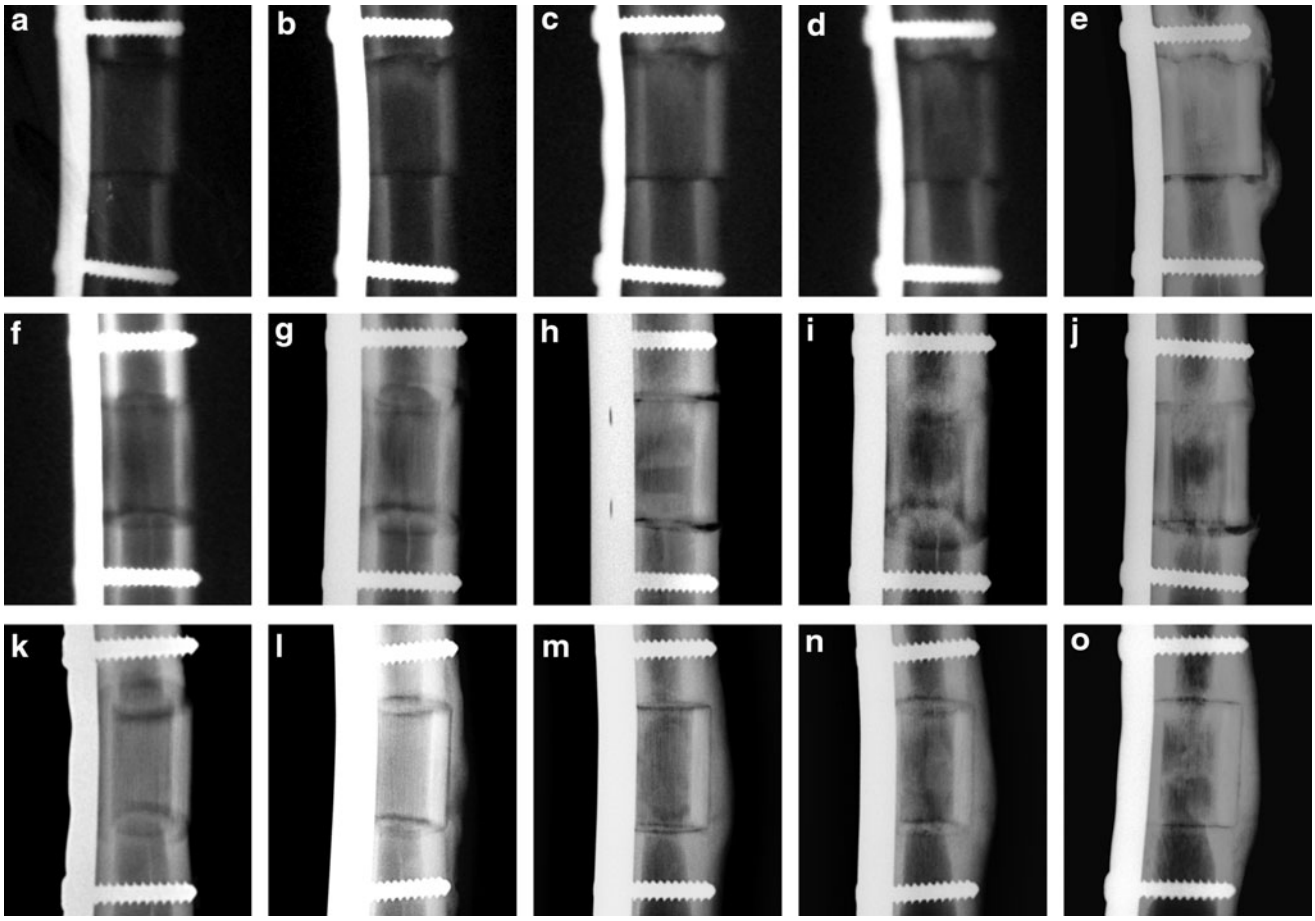

FIG. 5. Radiological images of periosteal callus presence and osteotomy healing at the proximal (upper) and distal (bottom) osteotomy line at 0 **(a, f, k)**, 4 **(b, g, l)**, 8 **(c, h, m)** 12 **(d, i, n)**, and 16 **(e, j, o)** weeks after surgery: BioSiC(HaCol) **(a–e)**; BioSiC(HaCol) + PRP **(f–j)**; and BioSiC(HaCol) + BMSCs **(k–o)**. PRP, platelet-rich plasma; BMSC, bone marrow stromal cell.

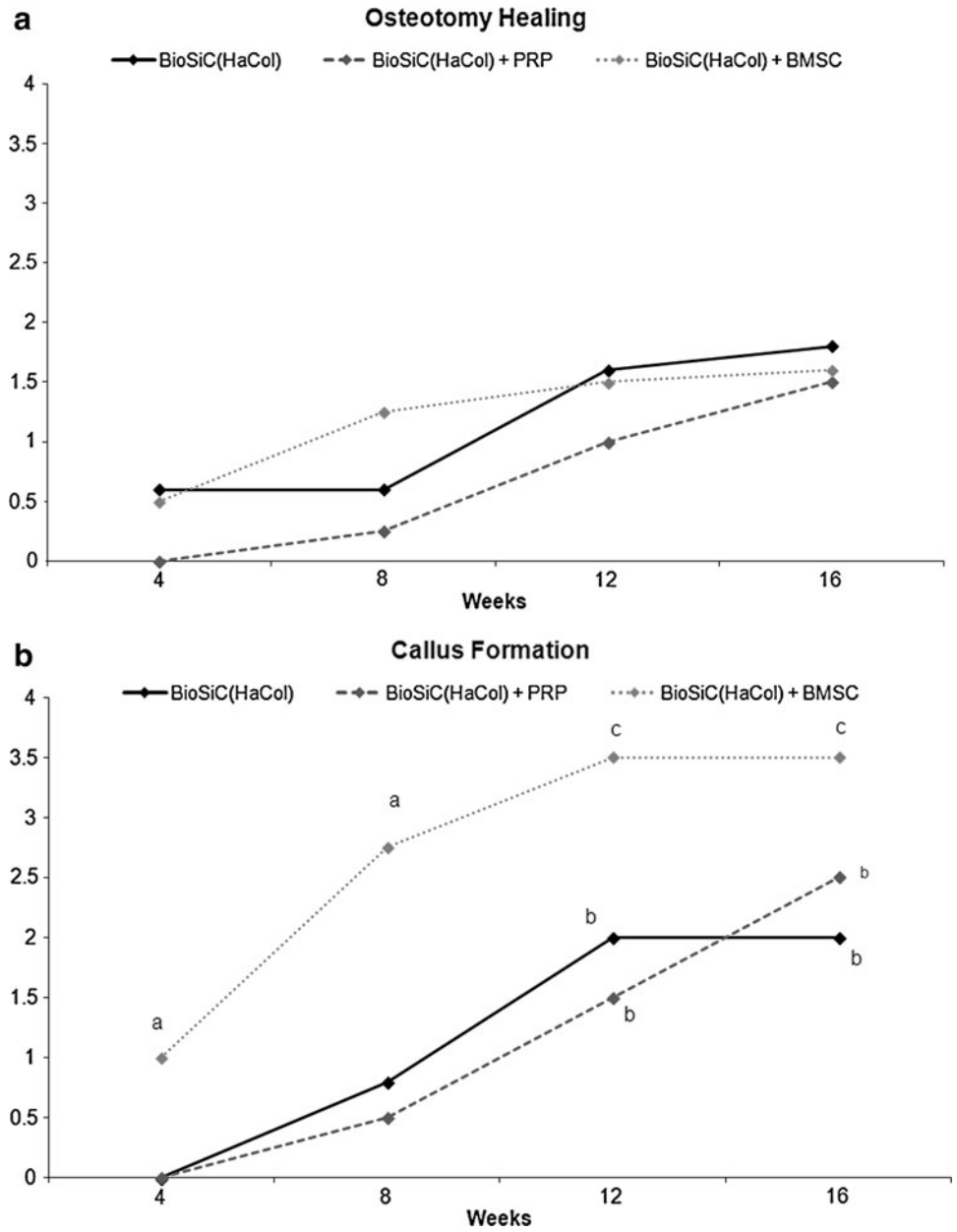

FIG. 6. Radiological score evaluation in terms of osteotomy healing **(a)** and periosteal callus presence **(b)** until 16 weeks after surgery. Dunnett *t*-test: periosteal callus presence: [a], BioSiC(HaCol) + BMSCs group versus BioSiC(HaCol) at 4 and 8 weeks ($p < 0.05$); [b], 12 and 16 weeks versus 4 weeks in BioSiC(HaCol) and BioSiC(HaCol) + PRP group ($p < 0.005$); [c], 12 and 16 weeks versus 4 weeks in BioSiC(HaCol) + BMSCs group ($p < 0.05$).

to-implant contact revealed significantly higher values in BioSiC(HaCol) + BMSCs when compared with BioSiC(HaCol) alone and BioSiC(HaCol) + PRP ($p < 0.005$). With regard to the new bone growth inside scaffold, BioSiC(HaCol) + BMSCs and BioSiC(HaCol) + PRP highlighted significantly higher value in comparison to BioSiC(HaCol) alone ($p < 0.005$ and $p < 0.05$ respectively).

Discussion

This study showed the safety, feasibility, and potential of this scaffold *in vivo* in a sheep model, as shown by radiological, histological, and histomorphometrical evaluations. In all tested treatments these analyses highlighted the presence of newly formed bone at the bone scaffolds interface. In particular, BioSiC(HaCol) + BMSC showed the highest value of bone-to-implant contact and new bone growth inside the scaffold. Hence, the obtained results have shown the potential of this scaffold in particular when combined with BMSCs.

During the last decades, a variety of scaffolds have been developed, and launched in the market, in order to face the increasing need for bone substitutes.[47–53] To date, acceptable clinical results have been obtained but no suitable solutions have been found as yet for regenerating long and load-bearing bone segments: Indeed, the mechanical strength of a highly porous but "disorganized" scaffold is often insufficient in order to manage the *in vivo* stresses and physiological loadings. So far, the development of three-dimensional synthetic systems with hierarchical architecture have been limited by the currently available processing technology.[54,55]

In recent years, material scientists have focused their attention on natural structures (e.g., shells, nacre, and wood, plants) and to their astonishing mechanical properties, generated by the complex and hierarchical organization of their

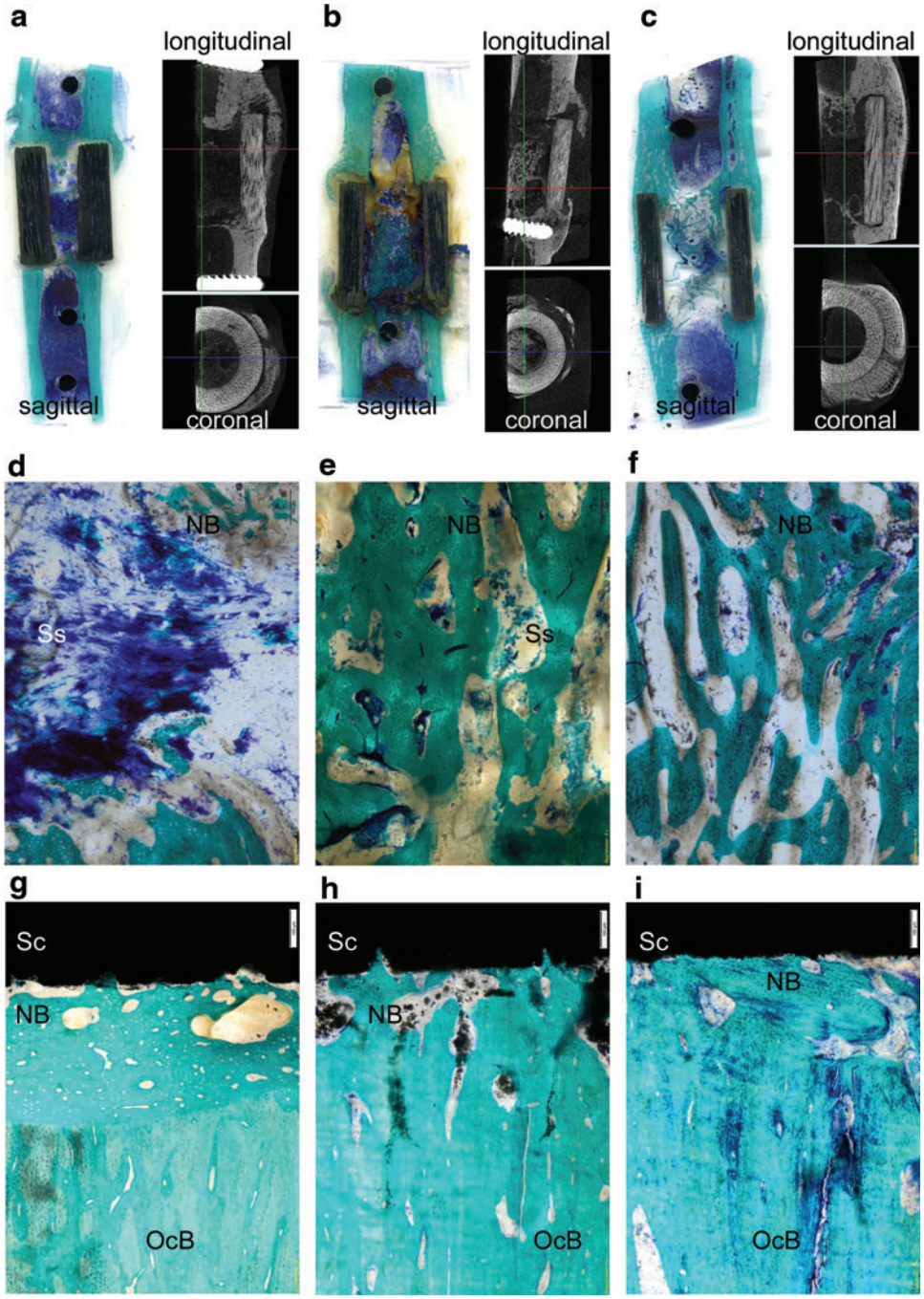

FIG. 7. Histological images showing bone osseointegration and newly formed bone tissue: BioSiC(HaCol) **(a, d, g)**; BioSiC(HaCol) + PRP **(b, e, h)**; and BioSiC(HaCol) + BMSCs **(c, f, i)**. Toluidine Blue, Acid Fuchsin, and Fast Green staining. Magnification: **(a–c)**, 1×; **(d–f)**, 4×; **(g–i)**, 20×. **(a–c)** Histological (sagittal) and microtomographic (longitudinal and coronal) images by Scanner Epson 2480 and Skyscan 1172 system (100 kV, 100 μA, 0.5 mm aluminum filter, software NRecon v.1.6.2.0), respectively. **(d–f)** Histological images of bone growth inside the bioactive HaCol core of the scaffold; **(g–i)** cortical bone contact to the biomorphic shell made of BioSIC. NB, new bone; OcB, old cortical bone (calcified bone stains a bright green); Sc, cortical-like scaffold; Ss, spongy-like part scaffold (blue or light brownish). Color images available online at www.liebertpub.com/tea

Table 1. Histomorphometric Results for the Three Groups of Treated Sheep (Mean ± SD)

Scaffold parameter	*BioSiC(HaCol)* (n = 5)	*BioSiC(HaCol) + PRP* (n = 4)	*BioSiC(HaCol) + BMSC* (n = 4)
Bone-to-implant contact (%)	15.0 ± 2.6	14.9 ± 2.8	26.8 ± 3.7[a]
New bone growth outside scaffold (%)	11.6 ± 4.2	15.1 ± 5.0	14.4 ± 4.6
New bone growth inside scaffold (%)	26.8 ± 3.7	38.5 ± 5.8[b]	41.1 ± 4.6[c]

Scheffé *post hoc* multiple comparison test.
[a]BioSiC(HaCol) + BMSC versus BioSiC(HaCol) and ($p < 0.005$).
[b]BioSiC(HaCol) + PRP versus BioSiC(HaCol) ($p < 0.05$).
[c]BioSiC(HaCol) + BMSC versus BioSiC(HaCol) ($p < 0.005$).
PRP, platelet rich plasma; BMSC, bone marrow stromal cell.

structure.[56] Woods have a porous structure similar to that of bone;[57] consequently, they manifest similar properties, that is, high elasticity, lightness, and strength. The conversion of woods into inorganic devices with complex morphology (i.e., biomorphic transformation) has been attempted for the past two decades.[58–60] Processes to convert natural woods into biomedical devices were carried out and optimized, thus leading to the development of BioSiC[16,17,61–68] a biocompatible ceramic which can be developed starting from different raw materials, that is, ligneous sources (e.g., red oak, sipo), so as to exhibit different complex microstructure and porosity. In particular, BioSiC obtained by transformation of hard woods is characterized by high strength that is able to sustain strong mechanical loads and porous morphology which is able to promote cell adhesion and attachment (see also Fig. 1a–e).[43]

A similar approach to reproduce the spongy part of bone has been carried out for the past decade, by reproducing in a laboratory the biomineralization processes that *in vivo* lead to the formation of new bone tissue.[21,69] In this regard, hybrid hydroxyapatite/collagen composites were developed, where the mineral phase was heterogeneously nucleated on the self-assembling collagen fibers in a specific manner, due to several control mechanisms (i.e., chemical, physical, morphological, and structural) acting at different dimensional ranges, from the molecular up to the macroscopic scale.[43] This led to the development of commercial products (i.e., RegenOss®, MaioRegen®) for the regeneration of bone and osteochondral tissues.

In the present work, in order to achieve high mimesis of the chemico-physical, morphological, and mechanical features of natural bones, hence to promote the formation of new tissue, the two products were combined to develop a bi-layered, bi-phasic bone-mimicking scaffold.[19]

The study also documented another important aspect for further increasing the tissue regeneration potential: the beneficial effects of a cell–scaffold combination. The concept of providing a combination of the key elements for tissue healing (an osteoconductive matrix, osteogenic cells, and growth factors) is well accepted in the scientific community: In fact, no single approach can successfully meet all the demands of bone regeneration alone.[70] The creation of viable bone tissue equivalent is facilitated by providing metabolically active cells that are able to contribute through their continuous matrix synthesis. While there is still no unanimous agreement on the most suitable cell type, preclinical *in vivo* studies have proved the positive effects of cells on bone regeneration, and promising findings have also been reported from human applications.[3,71,72]

The results of this study gave us clear indications with regard to the potential of combined implantation procedures. In fact, both the use of MSCs through the application of a bone marrow concentrate and platelet-derived growth factors were tested, and we clearly demonstrate the lack of substantial effect of PRP on one hand, and the improved results with the combined use of BMSCs and the new scaffold on the other hand.

The findings of this study suggest the potential of bioceramization processes that are applied to vegetable hierarchical structures for the production of new wood-derived bone scaffolds with good biological and mechanical properties, and document a suitable augmentation procedure in enhancing bone regeneration, particularly when combined with BMSCs. After this promising preliminary experience, future studies are needed to evaluate whether different scaffold prototypes, in terms of mechanical and biological properties, could further improve this bioengineered approach, thus developing the optimal cell-based scaffold strategy to be applied in a pilot study for enhancing bone regeneration process in humans.

Disclosure Statement

No competing financial interests exist.

References

1. Paderni, S., Terzi, S., and Amendola, L. Major bone defect treatment with an osteoconductive bone substitute. Chir Organi Mov **93,** 89, 2009.
2. Schieker, M., and Mutschler, W. Bridging posttraumatic bony defects. Established and new methods. Unfallchirurg **109,** 715, 2006.
3. Marcacci, M., Kon, E., Moukhachev, V., Lavroukov, A., Kutepov, S., Quarto, R., Mastrogiacomo, M., and Cancedda, R. Stem cells associated with macroporous bioceramics for long bone repair: 6- to 7-year outcome of a pilot clinical study. Tissue Eng **13,** 947, 2007.
4. Goldstrohm, G.L., Mears, D.C., and Swartz, W.M. The results of 39 fractures complicated by major segmental bone loss and/or leg length discrepancy. J Trauma **24,** 50, 1984.
5. Stevenson, S. The immune response to osteochondral allografts in dogs. J Bone Joint Surg Am **69,** 573, 1987.
6. Lord, C.F., Gebhardt, M.C., Tomford, W.W., and Mankin, H.J. Infection in bone allografts. Incidence, nature, and treatment. J Bone Joint Surg Am **70,** 369, 1988.
7. Mankin, H.J., Gebhardt, M.C., and Tomford, W.W. The use of frozen cadaveric allografts in the management of patients with bone tumors of the extremities. Orthop Clin North Am **18,** 275, 1987.
8. Alman, B.A., De Bari, A., and Krajbich, J.I. Massive allografts in the treatment of osteosarcoma and Ewing sarcoma in children and adolescents. J Bone Joint Surg Am **77,** 54, 1995.
9. Berrey, B.H., Jr., Lord, C.F., Gebhardt, M.C., and Mankin, H.J. Fractures of allografts. Frequency, treatment, and end-results. J Bone Joint Surg Am **72,** 825, 1990.
10. Mistry, A.S., and Mikos, A.G. Tissue engineering strategies for bone regeneration. Adv Biochem Eng Biotechnol **94,** 1, 2005.
11. Zhang, H., and Cooper, I. Aligned porous structures by directional freezing. Adv Mater **19,** 1529, 2007.
12. Deville, S., Jaiz, E., and Tomsia, A.P. Freeze casting of hydroxyapatite scaffolds for bone tissue engineering. Biomaterials **27,** 5480, 2006.
13. Tampieri, A., Celotti G., Sprio, S., Delcogliano, A., and Franzese, A. Porosity-graded hydroxyapatite ceramics to simulate natural bone. Biomaterials **22,** 1365, 2001.
14. Hadjidakis, D.J., and Androulakis, I.I. Bone remodeling. Ann N Y Acad Sci **1092,** 385, 2006.
15. Ingber, D.E. Cellular tensegrity: defining new rules of biological design that govern the cytoskeleton. J Cell Sci **104,** 613, 1993.
16. De Arellano-Lopez, A.R., Martinez-Fernandez, J., Gonzalez, P., Dominguez, C., Fernandez-Quero, V., and Singh, M. Biomorphic SiC: a new engineering ceramic material. Int J Appl Ceram Technol **1,** 56, 2004.

17. Gonzalez, P., Serra, J., Liste, S., Chiussi, S., Leon, B., Perez-Amor, M., Martinez-Fernandez, J., de Arellano-Lopez, A.R., and Varela-Feria, F.M. New biomorphic SiC ceramics coated with bioactive glass for biomedical applications. Biomaterials **24,** 4827, 2003.
18. Tampieri, A., Sprio, S., Ruffini, A., Celotti, G., Lesci, I.G., and Roveri, N. From Wood to Bone: multi-step process to convert wood hierarchical structures into biomimetic hydroxyapatite scaffolds for bone tissue engineering. J Mater Chem **19,** 4973, 2009.
19. Tampieri, A., Sprio, S., Ruffini, A., Martínez-Fernández, J., Torres Raya, C., Varela Feria, F.M., Ramírez Rico, J., and Harmand, M.F. Implants for "load-bearing" bone substitutions having hierarchical organized architecture deriving from transformation of vegetal structures. PCT/IB2011/054980, 2011.
20. Tampieri, A., Celotti, G., Landi, E., Sandri, M., Roveri, N., and Falini, G. Biologically inspired synthesis of bone like composite: self-assembled collagen fibers/hydroxyapatite nanocrystals. J Biomed Mater Res **67,** 618, 2003.
21. Sprio, S., Sandri, M., Panseri, S., Cunha, C., and Tampieri, A. Hybrid scaffolds for tissue regeneration: chemotaxis and physical confinement as sources of biomimesis. J Nanomater **2012,** 10, 2012.
22. Tampieri, A., Pressato, D., De Luca, C., Di Fede, S., and Landi, E. Cartilaginiform and osteochondral substitute comprising multilayer structure and use thereof. WO2006092718, PCT/IB2006/000452, 2006.
23. Landi, E., Tampieri, A., Sandri, M., Di Fede, S., and Pressato, D. A composite based on an apatite and a polysaccharide, method for its preparation and uses there of. WO2007045953, PCT/IB2006/002843, 2006.
24. Tampieri, A., Celotti, G., Roveri, N., and Landi E. Process to synthetize artificial bone tissue, artificial bone tissue obtained by such a process and use thereof. EP1447104, 2004.
25. Filardo, G., Madry, H., Jelic, M., Roffi, A., Cucchiarini, M., and Kon, E. Mesenchymal stem cells for the treatment of cartilage lesions: from preclinical findings to clinical application in orthopaedics. Knee Surg Sports Traumatol Arthrosc **21,** 1717, 2013.
26. Yin, D., Wang, Z., Gao, Q., Sundaresan, R., Parrish, C., Yang, Q., Krebsbach, P.H., Lichtler, A.C., Rowe, D.W., Hock, J., and Liu, P. Determination of the fate and contribution of *ex vivo* expanded human bone marrow stem and progenitor cells for bone formation by 2.3ColGFP. Mol Ther **17,** 1967, 2009.
27. Jäger, M., Hernigou, P., Zilkens, C., Herten, M., Li, X., Fischer, J., and Krauspe, R. Cell therapy in bone healing disorders. Orthop Rev (Pavia) **2,** 20, 2010.
28. Lieberman, J.R., Daluiski, A., and Einhorn, T.A. The role of growth factors in the repair of bone. Biology and clinical applications. J Bone Joint Surg Am **84,** 1032, 2002.
29. Liu, Y., de Groot, K., and Hunziker, E.B. BMP-2 liberated from biomimetic implant coatings induces and sustains direct ossification in an ectopic rat model. Bone **36,** 745, 2005.
30. Perut, F., Filardo, G., Mariani, E., Cenacchi, A., Pratelli, L., Devescovi, V., Kon, E., Marcacci, M., Facchini, A., Baldini, N., and Granchi, D. Preparation method and growth factor content of platelet concentrate influence the osteogenic differentiation of bone marrow stromal cells. Cytotherapy **15,** 830. doi: 2013.
31. Kon, E., Filardo, G., Di Martino, A., and Marcacci, M. Platelet-rich plasma (PRP) to treat sports injuries: evidence to support its use. Knee Surg Sports Traumatol Arthrosc **19,** 516, 2011.
32. Tschon, M., Fini, M., Giardino, R., Filardo, G., Dallari, D., Torricelli, P., Martini, L., Giavaresi, G., Kon, E., Maltarello, MC., Nicolini, A., and Carpi, A. Lights and shadows concerning platelet products for musculoskeletal regeneration. Front Biosci (Elite Ed) **3,** 96, 2011.
33. Cole, B.J., Seroyer, S.T., Filardo, G., Bajaj, S., and Fortier, L.A. Platelet-rich plasma: where are we now and where are we going? Sports Health **2,** 203, 2010.
34. Filardo G, Presti ML, Kon E, and Marcacci M. Nonoperative biological treatment approach for partial Achilles tendon lesion. Orthopedics **33,** 120, 2010.
35. Filardo G, Kon E, Pereira Ruiz MT, Vaccaro F, Guitaldi R, Di Martino A, Cenacchi A, Fornasari PM, and Marcacci M. Platelet-rich plasma intra-articular injections for cartilage degeneration and osteoarthritis: single- versus double-spinning approach. Knee Surg Sports Traumatol Arthrosc **20,** 2082, 2012.
36. Torricelli, P., Fini, M., Filardo, G., Tschon, M., Pischedda, M., Pacorini, A., Kon, E., and Giardino R. Regenerative medicine for the treatment of musculoskeletal overuse injuries in competition horses. Int Orthop **35,** 1569, 2011.
37. Weibrich, G., Hansen, T., Kleis, W., Buch, R., and Hitzler, W.E. Effect of platelet concentration in platelet-rich plasma on peri-implant bone regeneration. Bone **34,** 665, 2004.
38. Kon, E., Filardo, G., Delcogliano, M., Fini, M., Salamanna, F., Giavaresi, G., Martin, I., and Marcacci, M. Platelet autologous growth factors decrease the osteochondral regeneration capability of a collagen-hydroxyapatite scaffold in a sheep model. BMC Musculoskelet Disord **11,** 220, 2010.
39. Jensen TB, Rahbek O, Overgaard S, and Søballe K. Platelet rich plasma and fresh frozen bone allograft as enhancement of implant fixation. An experimental study in dogs. J Orthop Res **22,** 653, 2004.
40. Roldán, J.C., Jepsen, S., Miller, J., Freitag, S., Rueger, D.C., Açil, Y., and Terheyden, H. Bone formation in the presence of platelet-rich plasma vs. bone morphogenetic protein-7. Bone **34,** 80, 2004.
41. Mazor, Z., Peleg, M., Garg, A.K., and Luboshitz, J. Platelet-rich plasma for bone graft enhancement in sinus floor augmentation with simultaneous implant placement: patient series study. Implant Dent **13,** 65, 2004.
42. Fontana, S., Olmedo, D.G., Linares, J.A., Guglielmotti, M.B., and Crosa, M.E. Effect of platelet-rich plasma on the peri-implant bone response: an experimental study. Implant Dent **13,** 73, 2004.
43. Torres-Raya, C., Hernandez-Maldonado, D., Ramirez-Rico, J., Garcia-Gañan, C., de Arellano-Lopez, A.R., and Martinez-Fernandez, J. Fabrication, chemical etching, and compressive strength of porous biomimetic SiC for medical implants. J Mater Res **23,** 3247, 2008.
44. Lelli, M., Foltran, I., Foresti, E., Martinez-Fernandez, J., Torres-Raya, C., Varela-Feria, F.M., and Roveri, N. Biomorphic silicon carbide coated with an electrodeposition of nanostructured hydroxyapatite/collagen as biomimetic bone filler and scaffold. Adv Eng Mater **8,** 348, 2010.
45. Di Bella, C., Aldini, N.N., Lucarelli, E., Dozza, B., Frisoni, T., Martini, L., Fini, M., and Donati, D. Osteogenic protein-1 associated with mesenchymal stem cells promote bone allograft integration. Tissue Eng Part A **16,** 2967, 2010.
46. Parfitt, A.M., Drezner, M.K., Glorieux, F.H., Kanis, J.A., Malluche, H., Meunier, P.J., Ott, S.M., and Recker, R.R. Bone histomorphometry: standardization of nomenclature,

symbols, and units. Report of the ASBMR Histomorphometry Nomenclature Committee. J Bone Miner Res **2,** 595, 1987.
47. Bi, L., Jung, S., Day, D., Neidig, K., Dusevich, V., Eick, D., and Bonewald, L. Evaluation of bone regeneration, angiogenesis, and hydroxyapatite conversion in critical-sized rat calvarial defects implanted with bioactive glass scaffolds. J Biomed Mater Res A **100,** 3267, 2012.
48. Saini, R., Bajpai, J., and Bajpai, A.K. Synthesis of poly (2-hydroxyethyl methacrylate) (PHEMA) based nanoparticles for biomedical and pharmaceutical applications. Methods Mol Biol **906,** 321, 2012.
49. Martini, L., Staffa, G., Giavaresi, G., Salamanna, F., Parrilli, A., Serchi, E., Pressato, D., Arcangeli, E., and Fini, M. Long-term results following cranial hydroxyapatite prosthesis implantation in a large skull defect model. Plast Reconstr Surg **129,** 625, 2012.
50. Tschon, M., Fini, M., Giavaresi, G., Torricelli, P., Rimondini, L., Ambrosio, L., and Giardino, R. *In vitro* and *in vivo* behaviour of biodegradable and injectable PLA/PGA copolymers related to different matrices. Int J Artif Organs **30,** 352, 2007.
51. Giavaresi, G., Fini, M., Salvage, J., Nicoli Aldini, N., Giardino, R., Ambrosio, L., Nicolais, L., and Santin, M. Bone regeneration potential of a soybean-based filler: experimental study in a rabbit cancellous bone defects. J Mater Sci Mater Med **21,** 615, 2010.
52. Giavaresi, G., Tschon, M., Daly, J.H., Liggat, J.J., Sutherland, D.S., Agheli, H., Fini, M., Torricelli, P., and Giardino, R. *In vitro* and *in vivo* response to nanotopographically-modified surfaces of poly(3-hydroxybutyrate-co-3-hydroxyvalerate) and polycaprolactone. J Biomater Sci Polym Ed **17,** 1405, 2006.
53. Giavaresi, G., Branda, F., Causa, F., Luciani, G., Fini, M., Nicoli Aldini, N., Rimondini, L., Ambrosio, L., and Giardino, R. Poly(2-hydroxyethyl methacrylate) biomimetic coating to improve osseointegration of a PMMA/HA/glass composite implant: *in vivo* mechanical and histomorphometric assessments. Int J Artif Organs **27,** 674, 2004.
54. Ruiz-HItzky, E. Functionalizing inorganic solids: towards organic-inorganic nanostructured materials for intelligent and bio-inspired systems. Chem Rec **3,** 88, 2003.
55. Schieker, M., Seitz, H., Drosse, I., Seitz, S., and Mutschler, W. Biomaterials as Scaffold for Bone Tissue Engineering. Eur J Trauma **2,** 114, 2006.
56. Fratzl, P. Biomimetic materials research: what can we really learn from nature's structural materials? J R Soc Interf **4,** 637, 2007.
57. Fratzl, P., and Weinkamer, R. Nature's hierarchical materials. Prog Mater Sci **52,** 1263, 2007.
58. Rambo, C.R., and Sieber, H. Novel synthetic route to biomorphic Al2O3 ceramics. Adv Mater **17,** 1088, 2005.
59. Greil, P., Lifka, T., and Kaindl, A. Biomorphic cellular silicon carbide ceramics from wood: I. Processing and microstructure. J Eur Ceram Soc **18,** 1961, 1998.
60. Greil, P., Lifka, T., and Kaindl, A. Biomorphic cellular silicon carbide ceramics from wood: II. Mechanical properties. J Eur Ceram Soc **18,** 1975, 1998.
61. Gonzalez, P., Borrajo, J.P., Serra, J., Chiussi, S., Leon, B., Martinez-Fernandez, J., Varela-Feria, F.M., de Arellano-Lopez, A.R., de Carlos, A., Munoz, F.M., Lopez, M., and Singh, M. A new generation of bio-derived ceramic materials for medical applications. J Biomed Mater Res A **88,** 807, 2009.
62. Gonzalez, P., Borrajo, J.P., Serra, J., Liste, S., Chiussi, S., Leon, B., Semmelmann, K., de Carlos, A., Varela-Feria, F.M., Martinez-Fernandez, J., and de Arellano-Lopez, A.R. Extensive studies on biomorphic SiC ceramics properties for medical applications. Key Eng Mater **254–256,** 1029, 2003.
63. Varela-Feria, F.M., Ramirez-Rico, J., de Arellano-Lopez, A.R., Martinez-Fernandez, J., and Singh, M. Reaction-formation mechanisms and microstructure evolution of biomorphic SiC. J Mater Sci **43,** 933, 2008.
64. Martínez-Fernández, J., de Arellano-López, A.R., Varela-Feria, F.M., González-Fernández, P.M., Serra-Rodríguez, J.A., Liste-Carmueja, S., Chiussi, S., Pérez-Borrajo, J., Arias-Otero, J.L., León-Fong, B., and Pérez-Martínez, M. Material Biocompatible, Application Number P200203052 Spanish Patent, 2002.
65. Martínez-Fernández, J., de Arellano-López, A.R., Varela-Feria, F.M., González-Fernández, P.M., Serra-Rodríguez, J.A., Liste-Carmueja, S., Chiussi, S., Pérez-Borrajo, J., Arias-Otero, J.L., León-Fong, B., and Pérez-Martínez, M. Biocompatible Material, Application Number PCT/ES2003/000638 European Patent, 2003.
66. Martínez-Fernández, J., de Arellano-López, A.R., Varela-Feria, F.M., and Singh, M. Procedimiento para la fabricación de carburo de silicio a partir de precursores vegetales. Application Number P200102278, Spanish Patent, 2001.
67. Martínez-Fernández, J., de Arellano-López, A.R., Varela-Feria, F.M., and Singh, M. Procedure to fabricate silicon carbide ceramics from natural precursors. Application Number PCT/ES 02/00483, European Patent, 2002.
68. Martínez-Fernández, J., de Arellano-López, A.R., and Varela-Feria. Fabricación de cerámicas porosas y materiales multifásicos a partir de precursores celulósicos. Application Number P200800743, Spanish Patent, 2008.
69. Tampieri, A., Sprio, S., Sandri, M., and Valentini, F. Mimicking natural bio-mineralization processes: a new tool for osteo-chondral scaffold development. Trends Biotechnol **29,** 526, 2011.
70. Drosse, I., Volkmer, E., Capanna, R., De Biase, P., Mutschler, W., and Schieker, M. Tissue engineering for bone defect healing: an update on a multi-component approach. Injury **39(Suppl 2),** 9, 2008.
71. Petite, H., Viateau, V., Bensaïd, W., Meunier, A., de Pollak, C., Bourguignon, M., Oudina, K., Sedel, L., and Guillemin, G. Tissue-engineered bone regeneration. Nat Biotechnol **18,** 959, 2000.
72. Quarto, R., Mastrogiacomo, M., Cancedda, R., Kutepov, S.M., Mukhachev, V., Lavroukov, A., Kon, E., and Marcacci, M. Repair of large bone defects with the use of autologous bone marrow stromal cells. N Engl J Med **344,** 385, 2001.

Address correspondence to:
Elizaveta Kon, MD
Laboratory of Biomechanics
Rizzoli Orthopaedic Institute
v. Di Barbiano 1/10
Bologna 40136
Italy

E-mail: e.kon@biomec.ior.it

Received: February 11, 2013
Accepted: September 25, 2013
Online Publication Date: December 6, 2013